15th Australasian Fluid Mechanics Conference
The University of Sydney, Sydney, Australia
13-17 December 2004

An Experimental Study of the Jet of a Boat Propeller

A. Loberto[1], R.J. Brown[1], M.K. Kwek[1], A. Iida[2], H. Chanson[3], and S. Komori[4]

[1]School of Mechanical, Manufacturing, and Medical Engineering
Queensland University of Technology, Brisbane QLD 4001, AUSTRALIA

[2]Department of Mechanical Engineering, Kogakuin University
2665 Nakanomachi, Hachioji, Tokyo 192-0015, JAPAN

[3]Department of Civil Engineering
The University of Queensland, Brisbane QLD 4072, AUSTRALIA

[4]Department of Mechanical Engineering, Kyoto University
Kyoto 606-8501, JAPAN

Abstract

An experimental study of the velocity and concentration (scalar) fields of a propeller is presented. Field and laboratory measurements were undertaken. The former were up to 50 diameters downstream. Important findings were that the mean velocity and scalar fields quickly become Gaussian while further downstream they both become irregular sometimes approaching approximately linear profiles. Propeller turbulence causes rapid mixing giving an initial concentration dilution factor of 1/20,000 after fifty propeller diameters. Some preliminary comparisons with field measurements of an actual boat in a natural waterway are made. Considerably more work is needed to gain a full understanding of the complex problem of propeller mixing.

Introduction

In Queensland alone, boats and ships release approximately 4.5 ML of oil into marine environment each year, while this figure is about 1.0 million tonnes world wide [4]. In addition, significant quantities of unburned fuel, toxic combustion by-products and well over 14 M tonnes of antifouling agents (tri-butyl tin) are directly released into the water and dispersed by the vessels' propellers annually. Such pollutants have been shown to impact directly on Australia's coastlines, including the Great Barrier Reef. Inland waterways, dams, and estuaries are even more critically affected by pollution from vessels because dispersion is drastically limited by weak background flows and small water volumes. In all situations, propellers create considerable turbulence, which thoroughly mixes pollutants and chemicals into the water. It is of great importance to quantify pollutant concentrations in the jet region, and hence to estimate the effective contaminant concentrations emitted by vessels. Figure 1 shows a schematic diagram of dispersion of emissions in the propeller jet of a vessel. While there has been considerable research on propellers for ship propulsion, very little research has been done on the dispersing action of the propeller. We report results of the first study of its kind to experimentally quantify the dilution of a conserved scalar by a vessel type propeller. The present work aims to comprehend the fundamentals of mixing processes occurring in a propeller jet.

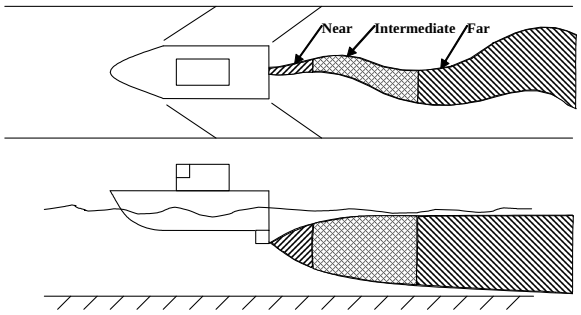

Figure 1: Schematic of boat propeller jet plume and regions of interest.

Experimental Method and Data Collection

New experiments were conducted to measure both the velocity and scalar concentration fields in a propeller jet. The introduced scalar was dye (Methylene Blue). No horizontal profile was performed because of experimental limitations, but flow visualisations indicated approximately horizontal symmetry of the flow field. Measurements were performed at several longitudinal locations ranging from near-field, x/D=2, to far-field, x/D=50, where x is the distance downstream of the propeller and D is the propeller diameter (tip-to-tip).

The tests were conducted in the closed loop flume of the Department of Mechanical Engineering at Kyoto University, Japan. The flume dimensions were 12 m (L) x 0.4 m (W) x 0.2 m (H). The water level was controlled by a sharp-crested weir at the channel downstream end. The water depth (h_1+h_2) was 0.150 m and held constant for all experiments (Fig. 2). The volume flow rate was held constant and resulted in a water surface velocity of 0.040 m/s, used for all experiments. The background turbulence intensity was low (rms/mean < 1%).

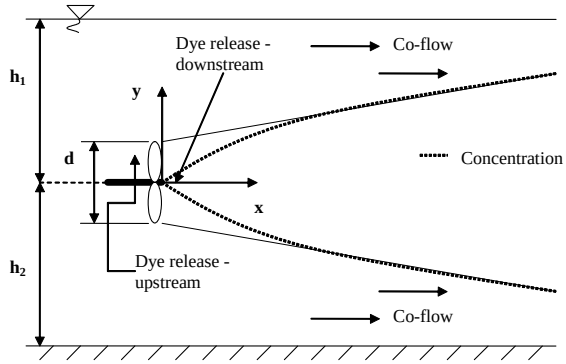

Figure 2: Schematic diagram of experimental set-up.

The experimental set up comprised a two-bladed propeller, powered by a variable speed electric motor with flexible cable transmission, held in space by a wing shaped frame where the long axis coincided with direction of flow. The propeller diameter, D was 20 mm. Velocity measurements were conducted with a 2D Dantec Laser Doppler Anemometer.

Dye concentrations (mean and fluctuations) were measured with a Komori concentration probe [5] held in place by an adjustable frame. The Komori probe has a sample rate of 1 kHz and a frequency response of up to 100 Hz. The data collection was conducted with a Sony PC208Ax digital recorder. The dye was released upstream of the propeller, 8 mm above the rotation axis and 4 mm upstream of the propeller blades (Fig. 2). The inside diameter of injection pipe was 1 mm. The flow of injected dye

was maintained constant by a syringe pump. Experimental conditions are shown in Table 1 listing initial dye concentration, C_o and injected flow rate, Q. The background concentration of dye steadily increased over time because the flume volume was fixed and the water was recirculated. The upward drift in background concentration was accounted for by measuring the background concentration in between each profile, about every thirty minutes. At each measurement point, the measured background concentration was subtracted from the reading to give the true concentration. Background fluctuations were eliminated by mixing the flow in a tank with an impeller. Spectral analysis was used to compare fluctuations in the flume before and after dye injection. No significant differences were observed even with relatively high background concentrations. The Komori probe exhibited a linear voltage response to variations in concentration. The probe was calibrated in clean water (0 ppm) and in solutions of known concentration up to the maximum range of the instrument (8 ppm).

The total experimental campaign consisted 600 point measurements. At each point, 120,000 instantaneous measurements were recorded with a sampling rate of 1 kHz. The data were processed by a FORTRAN program to obtain the concentration statistics, including the first four moments of the scalar concentration, although the paper focuses on mean concentration results. Velocity and scalar experiments were conducted separately.

x/D	Co	Q	Sample time
	ppm	mL/min	minutes
2	4000	5	2
10	4000	10	2
20	25000	10	2
50	25000	10	2

Table 1: Experimental conditions for upstream dye injection at 3000 rpm.

Velocity field

The mean velocity field was recorded in the longitudinal and tangential axes from x/D = 2.5 to x/D = 50 for two propeller speeds, 1500 and 3000 rpm. Downstream of the propeller, the evolving jet can be represented by a Gaussian profile once it is established [1]. Typical results are shown in Figure 3 for 3000 rpm. The data have been presented in a normalised format to emphasise jet flow field evolution. The data are compared with the Gaussian equation:

$$\overline{U} = U_m \exp\left[-\frac{1}{2}\left(\frac{r-r'}{\sigma}\right)^2\right] \quad (1)$$

as used by Brown and Bilger [2] for a study of reactive plumes in grid turbulence where U_m, r, r' and σ, are the maximum jet velocity, radial distance from centreline (shown as y on the figures), radial offset of curve centerline from x=0 and standard deviation of Gaussian profile, respectively. Overbars represent mean for velocity. Gaussian curves were fitted (with a least squares criteria) to the data, using a steepest descent, unconstrained multivariable curve fitting procedure. Equation (1) was chosen because it comprised fundamental parameters that are clear descriptors of the jet shape.

A power law was fitted to σ obtained from Eq (1) (Fig. 4, Table 2):

$$\frac{\sigma}{D} = k\left(\frac{x}{D}\right)^m \quad (2)$$

and a similar expression for decay of U_m:

$$\frac{U_m}{U_p} = k\left(\frac{x}{D}\right)^m \quad (3)$$

where U_p is the jet velocity immediately downstream of the propeller.

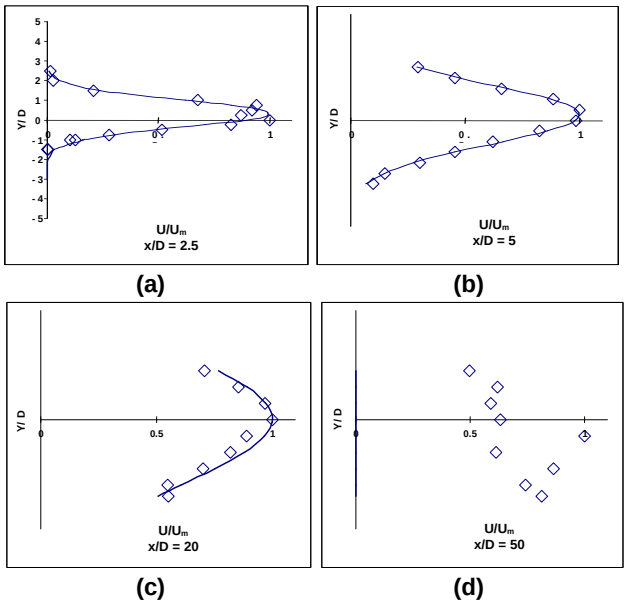

Figure 3: Mean velocity field $\overline{U}/U_m$ at 3000 rpm with profiles from Eq (1); (a), (b), (c), (d): x/D = 2.5, 5, 20, 50, respectively.

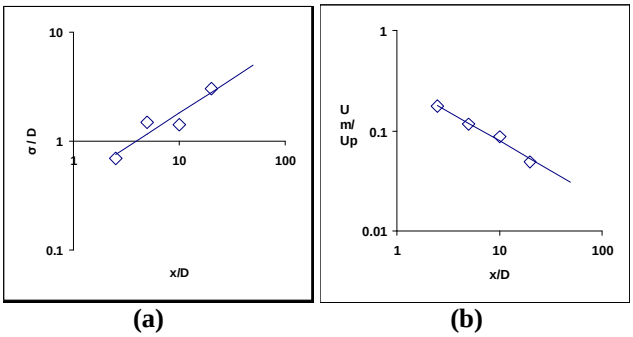

Figure 4: Evolution of Gaussian Profile statistics for mean velocity at 3000 rpm: (a), standard deviation; (b) mean.

At 3000 rpm, the jet velocity data exhibited some scatter in relation to the Gaussian profile. In particular, at the farthest downstream position (x/D=50), the velocity data exhibited a breakdown in jet profile whereas a slower jet (1500 rpm, results not shown) maintained a Gaussian distribution. There are a few likely causes of jet breakdown in this far field. It is conceivable that the jet was interacting with the wall. It is important to note that both jets shared a same rate of spread and that the jet did not break down in the far-field at 1500 rpm, although it touched the walls somewhat. Hence the evidence available did not support some jet impingement on the flume wall. The writers hypothesise instead that the higher velocity and flow of the 3000 rpm jet may have induced some instabilities leading to the jet break down observed at 3000 rpm. This matter is under further investigation.

Scalar Concentration Field

Since it was shown that submerged jets exhibit a Gaussian velocity profile ([1] and present study), the distributions of

conserved scalar were compared also with Gaussian curves using a similar method to Eq (1):

$$C = C_p \exp\left[-\frac{1}{2}\left(\frac{r-r'}{\sigma}\right)^2\right] \quad (4)$$

where C and C_p are the concentration at a point $P(x,r)$ and peak concentration, respectively.

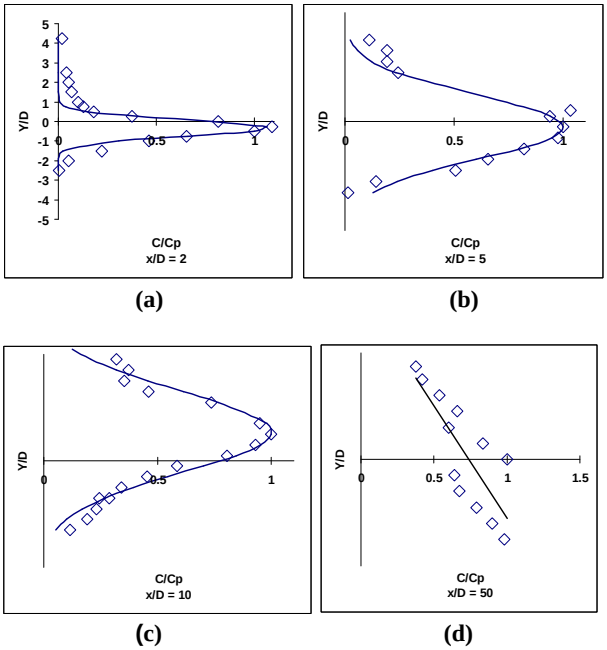

Figure 5: Vertical profiles of normalised mean centreline concentration at 3000 rpm.

Figure 5 shows vertical profiles for consecutive downstream locations, for x/D=2, 5, 10 and 50. The downstream location, x, and the radial location, y, are normalised against propeller diameter, D. Concentration, C, is normalised with the peak Gaussian concentration, C_p.

Drift of the plume centerline, r' has not been subtracted from the data so the reader can see the variability of the experiment. The maximum drift was less than D for all experiments. Despite some scatter, most data (Fig. 5a,b,c) compared favourably with Equation (4). Yet there were two obvious experimental variables that contributed to data scatter. Both were addressed through careful experimental procedure and post-processing of the results. First, the calibration of concentration probe was prone to drift, as expected of high frequency measuring probes. The calibration was re-checked over consistent periods in time during the experiment and systematic data were available to make corrections during the processing phase. Second, the background concentration of dye increased with time. Although the background concentration was measured periodically, the inherent randomness of the process and the limiting resolution of the equipment contributed toward some data scatter that could not be completely accounted for.

The evolution of dye concentration plume is of significant interest. Figure 5 illustrates that the plume originated, in the near-field region, with an approximately Gaussian shape (Fig. 5a) and evolved by outward spreading, eventually developing into an approximately linear distribution (Fig. 5d). The initial Gaussian shape was expected, based on previous results of near-field propeller jet. However, the observed linear profile in the far field (x/D=50) was a new finding. It is hypothesised that greater longitudinal dispersion of dye took place in the high-velocity flow region next to the free-surface, while, next to the bottom, dye transited at lower flow velocities in the boundary layer, hence with a higher concentration. The influence of swirl may also contribute to this effect. Indeed the data showed that, next to the bottom, the scalar concentration was approximately fifty per cent larger than that next to the free surface (Fig. 5). Such a result would be amplified in a rough, coarse natural channel leading possibly to a greater concentration gradient between lower and upper flow regions.

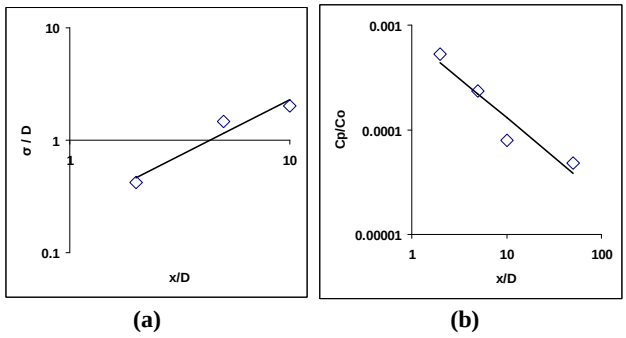

Figure 6: Evolution of Gaussian profile statistics for mean concentration; (a) standard deviation, σ; (b) mean on centreline, Cp.

	Velocity		Scalar	
	σ/D	U_m/U_p	σ/D	C_p/C_o
m	0.63	-0.59	1.00	-0.76
k	0.42	0.31	0.23	7.40E-04

Table 2: Coefficients for line of best fit for axial change of mean velocity and mean scalar concentration at 3000 rpm corresponding to Figures 4 and 6, respectively.

Figure 6 shows the longitudinal variations of Gaussian profile properties, σ and C_p. The downstream change in radial offset of the plume (not shown) drifts by approximately one propeller diameter

Figure 6(a) shows the growth in plume width, σ, with increasing downstream distance, using a Log-Log scale. A power-law curve was fitted to the growth trend of σ/D:

$$\frac{\sigma}{D} = k\left(\frac{x}{D}\right)^m \quad (5)$$

The least squares fit was carried out to ascertain the magnitudes of the coefficients, k and m, where m is the gradient of the straight line in Figure 6(a) and k takes the value of 10^c where c is the y- intercept of the same straight line of best fit. The values of m and k are shown in Table 2.

Figure 6(b) shows the decay in peak concentration, C_p, with increasing downstream distance, using a Log-Log scale. As with Figure 6(a), a power-law curve was fitted to the growth trend of C_p/C_0:

$$\frac{C_p}{C_0} = k\left(\frac{x}{D}\right)^m \quad (6)$$

The values of m and k for best data fit in Figure 6(b) are shown in Table 2. The total dilution of the peak concentration is of

significant interest. In Figure 6(b), the peak concentration was reduced by a factor of 1.48E-6 (i.e. ~ 1/20,000) by x/D=50.

It should be noted that since the results at x/D=50 did not exhibit a Gaussian profile, the graphs in Figure 6(a) does not include data from this axial location. Furthermore, in Figure 6(b), for the data point at x/D=50, the measured data at the propeller centreline was used as an estimate of C_p since the profile exhibited did not allow a Gaussian profile to be fitted. It should also be noted that in Figure 6, graphs (a) and (b), both axes have been normalised against D.

Corresponding experiments with reduced propeller speed (1500 rpm) exhibited similar trends to the 3000 rpm results with an increased growth of σ and faster decay C_p. Further experiments with a dye release point downstream of the propeller and with the same propeller speed produced results (not shown) that supported those described above and shown in Figure 5 and Figure 6. The results from the downstream dye release showed a less pronounced shift of the centreline, a similar rate of change of plume width (although with slightly lower magnitudes) and similar decay rate of peak concentration. However, the difference in peak concentration between the free surface and bottom was more pronounced, with a three-fold change, fifty per cent higher than that exhibited by the upstream experiment.

Present results can be used to quantify the dispersion and mixing of scalars by a propeller. As shown in Figure 6(b) and Table 2, the decay exponent for C_p/C_0 is m=-0.76 in the range $2<x/D<50$. Such a result is lower than that for a plume for which m=-1 [2], but larger than that typically obtained for a jet. However, in the range $x/D<10$ the exponent m was considerably greater : i.e., m=-1.5, suggesting that the near flow field is characterised by a greater decay of peak concentration. Overall significant mixing occurs with a dilution of approximately 1/20,000 by x/D=50.

Field Experiment

In parallel with the present study a series of field tests [3] were conducted in cooperation with the Environmental Protection Authority and the University of Queensland to contribute to a broad environmental assessment of Eprapah Creek, Brisbane, which included: continuous water quality sampling, creek velocity measurements, bird and fish activity monitoring. All measurements were maintained for up to 8 hours continuously.

During the course of the field test several different outboard motor / boat combinations were driven past the sampling area at different load/velocity combinations which were carefully monitored. Boats with outboard motors were driven past the measurement point for a range of speeds and configurations. Figure 7 shows the effect of a non planing outboard motor on the velocity field at the point of measurement which was 0.5 m below the surface and approximately 1 m from the passing boat horizontally. The results in figure 7 showed high turbulence caused by both propeller and bow wave corresponding to that observed in the present study. These effects were detected in the turbulent velocity data for a period of less than one minute typically, but the velocity autocorrelation function showed some effects lasting at least eight minutes, while water quality observations showed some important levels of fluctuations for several minutes after boat passage (e.g. in terms of turbidity, conductivity and temperature [3]). Overall the data suggested some mixing induced by wake waves and by the propeller. Further comparison of the velocity and scalar fields in the laboratory and field are continuing.

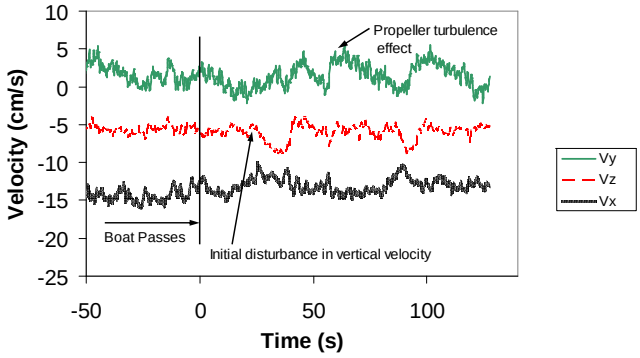

Figure 7: Instantaneous velocity disturbance caused by an outboard motor. (coordinates: x, y, z; parallel to creek, transverse, vertical, respectively.

Summary and Conclusion

The initial conclusion of this study of dye mixing by a propeller indicates that contaminant mixing is rapid giving a reduction in peak Gaussian concentration by a factor of 1.48E-6 after fifty propeller diameters. With an actual boat in a natural waterway, the situation will be different because the incoming velocity to the propeller will be higher and interactions with low level environmental turbulence will occur. Considerably more work is needed to gain a full understanding of the complex problem of propeller mixing.

Acknowledgments

We gratefully acknowledge the expert assistance of Dr K Nagata and Mr Y Ito, and staff in the conduct of these exeriments at Kyoto University. Support for Dr. Richard Brown under a Research Fellowship from the Japan Society for the Promotion of Science and the Australian Research Council is gratefully acknowledged.

References

[1] Albertson, M.L., Dai, Y.B., & Jensen, R.A., ***et al.***, Diffusion of Submerged Jets, in *ASCE Transactions* (Fort Collins, 1948, 639-664.

[2] Brown, R.J. & Bilger, R.W., An Experimental Study of a Reactive Plume in Grid Turbulence. *J Fluid Mech.*, **312**, 1996, 373-407.

[3] Chanson, H., Brown, R., Ferris, J., & Warburton, K., "A Hydraulic, Environmental and Ecological Assessment of a Sub-tropical Stream in Eastern Australia: Eprapah Creek, Victoria Point QLD on 4 April 2003", *Report No. CH52/03*, Dept. of Civil Eng., Univ. Queensland, Australia, 2003.

[4] Kelly, C.A., Ayoko, G.A. & Brown, R.J., Under Water Emissions from a 2-Stroke Outboard Engine: a Comparison between EAL and Equivalent Mineral Lubri-cant. *Proc 2nd Internl Conf on Tribology in Environ Design* 8th-10th September 2003, Bournemouth, UK., (Eds M. Hadfield & Y. Wang) ISBN: 1-86058-415-2,. 2003, 171-180

[5] Komori, S., Hunt, J.C.R., & Kanzaki, T., ***et al.***, The Effects of Turbulent Mixing on the Correlation between Two Species and on Concentration Fluctuations in Non-Premixed Reacting Flows. *J. Fluid Mech.*, **228**, 1991, 629-659.